석 사 학 위 논 문
Master's Thesis

VR 환경 내 물체 인식을 위한 다관절 정전기 브레이크 방식 웨어러블 햅틱 디바이스 개발

Development of a multi-joint electrostatic brake-based wearable haptic device for object recognition in VR environments

2024

와닛워라난 니샤 (Vanichvoranun, Nicha)

한 국 과 학 기 술 원

Korea Advanced Institute of Science and Technology

석 사 학 위 논 문

VR 환경 내 물체 인식을 위한 다관절 정전기 브레이크 방식 웨어러블 햅틱 디바이스 개발

2024

와닛워라난 니샤

한 국 과 학 기 술 원

문화기술대학원

VR 환경 내 물체 인식을 위한 다관절 정전기 브레이크 방식 웨어러블 햅틱 디바이스 개발

와닛워라난 니샤

위 논문은 한국과학기술원 석사학위논문으로
학위논문 심사위원회의 심사를 통과하였음

2024년 06월 11일

심사위원장 윤 상 호 (인)

심 사 위 원 우 운 택 (인)

심 사 위 원 윤 희 택 (인)

Development of a multi-joint electrostatic brake-based wearable haptic device for object recognition in VR environments

Nicha Vanichvoranun

Advisor: Sang Ho Yoon

A dissertation submitted to the faculty of
Korea Advanced Institute of Science and Technology in
partial fulfillment of the requirements for the degree of
Master of Science in Culture Technology

Daejeon, Korea
June 11, 2024

Approved by

Sang Ho Yoon
Professor of Graduate School of Culture Technology

The study was conducted in accordance with Code of Research Ethics[1].

[1] Declaration of Ethical Conduct in Research: I, as a graduate student of Korea Advanced Institute of Science and Technology, hereby declare that I have not committed any act that may damage the credibility of my research. This includes, but is not limited to, falsification, thesis written by someone else, distortion of research findings, and plagiarism. I confirm that my thesis contains honest conclusions based on my own careful research under the guidance of my advisor.

MGCT 와닛워라난니샤. VR 환경 내 물체 인식을 위한 다관절 정전기 브레이크 방식 웨어러블 햅틱 디바이스 개발. 문화기술대학원 . 2024년. 31+iv 쪽. 지도교수: 윤상호. (영문 논문)
Nicha Vanichvoranun. Development of a multi-joint electrostatic brake-based wearable haptic device for object recognition in VR environments. Graduate School of Culture Technology . 2024. 31+iv pages. Advisor: Sang Ho Yoon. (Text in English)

초 록

햅틱 장갑은 가상 현실(VR)에서 시각 정보와 함께 촉각 피드백을 제공함으로써 몰입감 있고 사실적인 물체와의 상호작용을 재현한다. 선행 연구는 손가락 끝이나 손 끝 관절에 피드백을 전달하는 데 중점을 두어 다른 손가락 마디는 연구가 아직 많이 진행되지 않았다. 본 연구는 모든 손가락 마디에 역감 피드백을 전달하는 햅틱 장갑을 제안하여 VR 환경에서 물체를 잡을 때 물체 모양을 더 정확하게 인식할 수 있도록 한다. 본 연구에서 개발한 이중 레이어, 다중 적층 정전기 클러치는 각 마디마다 정전기 브레이크를 형성하여 가볍고(130g) 높은 착용감과 사용성을 유지하면서도 세밀한 역감 피드백의 재현을 가능하게 한다. 사용자 실험 결과 본 연구 디바이스를 사용할 때 물체의 각을 재현하는 정확도와 해상도가 크게 개선되었으며, VR에서 다양한 형태의 물체와 상호작용할 때 현실감과 몰입감이 향상되었다.

핵 심 낱 말 햅틱, 가상 현실, 웨어러블 및 정전기 브레이크

Abstract

Haptic gloves allow for an immersive and realistic experience of interacting with objects in virtual reality (VR) by combining tactile sensations with visual information. Previous approaches concentrated on providing feedback to the fingertips or distal phalanges while paying little attention to the remaining phalanges. This idea proposes a haptic glove that provides force input to all finger areas, from fingertips to proximal phalanges, improving the perception of object forms during VR gripping activities. The designed double-layer and multi-stacked electrostatic clutches (ES clutches) function as an electrostatic brake (ES brake) for each phalanx, allowing for high-resolution force feedback in a lightweight structure (130 grams) that is nevertheless wearable and usable. Validation of user perception performance demonstrated significant improvement in the perception of phalanx angle positions and an overall enhanced experience of realism and immersion when interacting with objects of varying shapes in VR.

Keywords Haptics, Virtual Reality, Wearables, and Electrostatic Brake

Contents

Contents i
List of Tables ii
List of Figures iii

Chapter 1. Introduction **1**

Chapter 2. Related Works **3**
2.1 Haptic Interface for Shape Rendering in VR 3
2.2 Whole-Hand Haptic Feedback with Wearables 3
2.3 Electrostatic Clutch/Brake Applications in HCI 4
2.4 Key Improvements 4

Chapter 3. Electrostatic Clutch Operating Principal **6**

Chapter 4. System Overview **9**
4.1 Fabrication of Multi-Phalanx ES Brake 9
4.2 Hardware Implementation 11

Chapter 5. Technical Evaluation **12**
5.0.1 Fatigue Life 12
5.0.2 Force Feedback Validation 12

Chapter 6. Haptic Rendering with Electrostatic Brake Haptic Glove **14**
6.0.1 Exploratory Study 14
6.0.2 Haptic Rendering Algorithm 15

Chapter 7. User Study **17**
7.0.1 User Study 1: Phalanx-Angle Position Perception 17
7.0.2 User Study 2: Object Perception Experience 19

Chapter 8. Applications **22**

Chapter 9. Discussion **24**

Chapter 10. Conclusion **25**

Bibliography **26**

List of Tables

2.1 The purposed haptic gloves' performances in comparison with the similar previous works . 5

List of Figures

3.1 Operating principle of ES clutch used in the haptic glove. (a) Top and bottom strips freely slide over the middle strip when there is no difference of electrical potential (0 V). (b) When the voltage (>300 V) is applied, electrostatic adhesion occurs to lock between layers. (c) Multiple ES brakes to provide force feedback to each phalanx. 6
3.2 Friction force measured for applied voltage between 100 V and 1000 V. The initial overlap area was 10cm^2 and the pulling speed was around 0.5 mm/s. 7

4.1 ES brake structure and components. (a) ES brakes are connected to all phalanges. (b) A single ES brake includes two aluminum electrode strips and a sliding strip to form an overlap area of 10 cm^2. 10
4.2 Overview of haptic glove prototype and components. 10
4.3 Multi-phalanx ES brake system flow. ES brakes and LRAs are employed to create force and tactile sensation. The control circuit and portable high-voltage supply enabled force feedback sensation on multiple phalanges. 11

5.1 ES brake transferred force to each phalanx for 3 different wrist anchoring forces (1.5 N, 3 N, and 5 N). ES brake provided a maximum of 12 N (350 VAC with 10 Hz and an overlap area of 10 cm^2. 12

6.1 The result of an exploratory study on force localization perception accuracy with the proposed device. (a) Identification accuracy when a single braking point is applied at a single phalanx, (b) Perceived force feedback location distribution when multiple braking points are applied at multiple phalanges. 15
6.2 Designated haptic rendering patterns for applying ES brake(s) (blue dots) to stimulate various force feedback patterns (red dots). 15
6.3 Haptic rendering pipeline. Haptic rendering patterns from the exploratory study were employed to support force feedback on multiple phalanges for the index, middle, and thumb. 16

7.1 Finger phalanx-angle positions perception test study setup. (a) Bending all phalanges together for 5 different levels (2, 4, 6, 8, 10 levels) and (b) bending DP & IP together, while PP was fixed for 4 different levels (2, 4, 6, 8 levels). Both (a) and (b) contained no activation condition as well (0 level). 17
7.2 The average identification accuracy of the phalanx-angle positions perception test. (a) The comparison of identification accuracy between all-phalanges and DP-only activation conditions when all phalanges are bending together and (b) the identification accuracy of all-phalanges activation condition when bending DP and IP while PP is fixed. The error bars represent standard errors. 18
7.3 Object perception study with sphere, quadrangular prism, triangular prism, and cylinder using 3 haptic feedback conditions including (a) DP-only activation, (b) all-phalanges activation, and (c) all-phalanges with adaptive activation. 20

7.4 The object perception experience ratings for various haptic feedback conditions. Each bar graph refers to the subjective rating from the participant under five criteria including realism, comfort, immersion, harmony, and satisfaction. 21

8.1 Example use case scenarios showing (a),(b) industrial applications and (c),(d) personal application. 22

Chapter 1. Introduction

Grasping allows us to complete activities with objects by using their features, such as shape, size, and stiffness. In VR, gripping perception is vital in generating immersive and realistic experiences that enhance the sense of presence and engagement [1, 2]. Users might then manipulate virtual items at the same level as they would in the physical world. Haptic gloves have been created to provide a realistic sense of gripping when engaging with virtual objects in various applications such as teleoperation [3] and rehabilitation [4]. Some of these gloves combine vibrotactile and force feedback to create a grasping sensation.

Haptic gloves have recently concentrated on providing force feedback on the fingertip in the area of distal phalanges (DP) [5]. Researchers generally ignore rendering forces on intermediate (IP) and proximal (PP) phalanges due to the hardware complexity and device footprint required by motors and pneumatic systems. Attaching many components to the hand might cause discomfort over time and inhibit natural hand movements. Furthermore, it has not been investigated if rendering force feedback across several phalanges improves object perception in VR. Recent work adopted a lightweight and high power-to-size ratio technique employing Shape Memory Alloy (SMA) [6]. However, it lacks responsiveness to provide dynamic force feedback. As a result, it is critical to build lightweight gear that provides force feedback for all phalanges.

The concept of the ES clutch [7, 8] has been applied in recent works. Unlike conventional clutches, which frequently rely on mechanisms like interlocking teeth or magnetic forces, ES clutches use electrical forces to prevent movement. When these clutches are engaged, their two high-dielectric layers provide electrostatic adhesion. The motion between the surfaces is then stopped by these clutches. Previous works used ES clutches for exoskeleton [9], haptic gloves [10, 11], and sleeves [12], given their thin, light structure and low power consumption. Nevertheless, single-node force feedback was the primary focus of earlier methods, which is inadequate to offer a complete grasping experience on the hand.

Previous works extended the haptic interface with multi-finger [13] and multi-point [14] force feedback with the hand for promoting a full grasping sensation. However, there are drawbacks to their work, such as low blocking force and system responsiveness. Furthermore, a number of haptic rendering techniques have been proposed to navigate the hardware constraints. Prior research, for instance, focused on synchronizing the haptic feedback and visual content during grasping. The fundamental haptic device needs and perceptual thresholds for emulating grasping sensations were also investigated. However, the majority of haptic rendering solutions focused on collision-based actuation for the fingertips, which limits rich feedback sensation and necessitates heavy computation. Therefore, more investigation is needed to find the best way to grip VR objects with the complete finger, and it is important to validate the understanding of how the fundamental functions of human perception.

This work suggests using wearable haptic feedback to provide force feedback to each finger phalanx. In substitution for PVDF-HFP (Poly(vinylidene fluoride-co-hexafluoropropylene)), which was employed in earlier studies [15, 16], PVDF (Polyvinylidene Fluoride)) was utilized. Higher mechanical strength, electric constant, and flexibility are all made possible by this material, which results in a longer activation cycle and a quicker release time. Furthermore, in accordance with [5], linear resonant actuators (LRA) were incorporated to produce a rich tactile feedback experience. An investigation of how humans perceive localized force at different phalanges was carried out. A haptic rendering technique for multi-phalanx

force feedback was created based on the findings. Additionally, the effectiveness of the haptic glove in determining phalanx angle positions and evaluating realism during grasping activities was assessed by a user study.

The contributions of this work are as follows:

- Development of wearable force feedback that can apply force to all regions of the finger with high energy efficiency (12 N with 6 mW) while maintaining the lightweight structure (130 grams);
- The formation of a haptic rendering algorithm and guidelines for the effective and efficient operation of a multi-phalanx electrostatic brake;
- Examining how force rendering affects object perception through technical assessments and user tests; and
- Providing examples of how the suggested multi-phalanx electrostatic brake improves haptic experiences.

Chapter 2. Related Works

2.1 Haptic Interface for Shape Rendering in VR

Several haptic feedback techniques have been developed in earlier research to render the shape of VR objects. In this instance, researchers focused on simulating the skin sensation by creating a sense of touch/contact through skin stretching, compressing, vibrating, and poking [17–19]. These works employed a mobile haptic feedback platform operated with small motors and a linkage mechanism to stimulate the fingertip. Moreover, other works employed linear resonant actuators (LRAs) [20] and pneumatic pin arrays [21, 22] to enhance cutaneous sensation with vibration and physical displacement with wearable form factor. Although these methods supported numerous sensations related to VR objects' shape and texture [23], the absence of kinesthetic force feedback prevents them from aligning the gripping feeling with VR situations. For example, fingers contact each other while grasping objects or provide a similar haptic sensation for various multilateral shapes.

Force feedback or kinesthetic feedback devices have been suggested in order to restrict or move the hand (or fingers) to render shape during grasping [24]. Early kinesthetic haptic feedback devices were primarily stationary form factors that required a large physical footprint but supported a full 6-DOF control with 3-DOF force feedback [25–27]. For force feedback rendering research, these devices have been used to generate realistic and high-fidelity haptic feedback with 3D objects [28]. With the advancement of hardware components, researchers started to adopt the force feedback to smaller form factors while meeting minimal force feedback requirements.

Researchers started to develop diverse haptic interfaces for shape rendering with compact and portable form factors including handhelds and wearables. Prior works suggested handheld controllers with integrating pin-based display for 2.5D shape rendering [29], a spinning wheel to render textures [30], combining mechanical brake and voice coil actuators for simulating weight and grasping [31], and expandable rings for grasping [32]. Although these devices were ungrounded, they still required users to hold or be in contact with a controller which prevents natural hand interactions.

To this end, wearable form factors like gloves or wristbands have been suggested to support realistic haptic feedback sensation while allowing natural hand interactions [33]. By directly applying haptic feedback to one's own hand, these works enable realistic and immersive user experience with VR objects. In general, haptic gloves were equipped with actuators and force feedback mechanisms distributed across the fingers [34], palm [35], and wrists [36] to promote natural grasping and manipulating sensation in VR. This work further extends the capability of the wearable haptic interface to promote grasping sensation with a novel kinesthetic force feedback.

2.2 Whole-Hand Haptic Feedback with Wearables

The hand has been highlighted as a main body part to apply diverse forms of wearable haptic feedback to promote enhanced object perception [37] and task performance [38–40]. For object perception, previous works included kinesthetic haptic feedback as a main feedback method [41] since force is an essential element for the human to acquire shape perception [42]. Kinesthetic feedback generally comprises active and passive actuations. Here, the active force feedback provides active motion and

resistance force, while the passive approach only offers resistance force like braking. Although haptic gloves with active actuations using cable-driven [43, 44], tendon-driven [45], pneumatic pump [46], shape memory alloy [6] and twisted-string actuator (TSA) [47] supported realistic force rendering, they exhibit significant drawbacks due to the required power consumption, hardware complexity, and large footprint.

Hence, recent works have focused on implementing compact and highly efficient passive force feedback by supporting only braking forces. Passive force feedback has advantages over the active approach in terms of fewer hardware requirements and a safer user environment. Previous works utilized magnetorheological (MR) fluid [48, 49], cable-locking [50, 51], pneumatic jamming [52], eddy-current [53], pawl & ratchet [54], and electrostatic adhesion [5] to resist motion from body parts utilizing various mechanisms. Still, these works support kinesthetic feedback in a single-node fashion. For example, braking force was transferred to either DP, IP, or PP for haptic gloves [55]. This work aligns with ongoing passive kinesthetic force feedback, primarily utilizing a braking mechanism for efficient operation. Moreover, multi-phalanx force feedback is enabled in each fingertip, and a method to render passive force feedback to a multi-phalanx configuration is proposed to enhance object perception.

2.3 Electrostatic Clutch/Brake Applications in HCI

ES clutch has been suggested with the advantages of enabling passive force feedback in thin layers and lightweight form factors while maintaining performance reliability [7]. Previous works applied various operating mechanisms and designs to employ electrostatic adhesion in wearable form factors. These include clutch with simple moving strips [56], rubber-spring [8], stretchable textile with moving strip [12], liquid-metal surface [57], all-fabric type [58], and spring-attached pulley [11]. These approaches achieved seamless integration with wearables, enhanced user comfort, and created high-force density.

With these advantages, HCI researchers have started to employ and utilize ES clutches/brakes for interaction purposes. Researchers initially utilized electrostatic adhesion to improve the grasping performance in VR [5, 15]. Here, the authors successfully demonstrated the grasping performance improvement by minimizing finger-object generation using a clutch along with vibration. Subsequent work expanded the scope of applying ES brake to whole-body garments level [9]. Moreover, the electrostatic adhesion used in the ES brake was also utilized to stimulate variable friction of surfaces for enhanced interactions [59, 60]. This work further expands the capability of the electrostatic braking mechanism by further minimizing the footprint while maintaining the amount of force feedback with a multi-layer configuration. This also allows us to provide a faster release upon deactivation of electrostatic adhesion.

2.4 Key Improvements

As depicted in Table 2.1, the proposed haptic device introduces several key improvements over previous designs, enhancing its practicality and performance. Firstly, it significantly reduces power consumption, requiring only 6 mW per actuator, which is markedly lower than many existing devices such as the 20 W used in the 4-DOF portable haptic interface. This makes the device more energy-efficient and suitable for extended use. Secondly, the device offers a substantial increase in maximum blocking force, achieving 30 N. This is a significant enhancement compared to the 2 N and 20 N forces seen in some earlier designs, ensuring stronger and more realistic force feedback. Additionally, unlike some previous haptic devices that only provide feedback to specific parts of the finger, this device covers all finger regions comprehensively, offering a more immersive and detailed haptic experience. Finally, the

device balances activation and deactivation responsiveness effectively, with both occurring in under one second. Although not the fastest in terms of activation time, which is measured in milliseconds in some other devices, this balanced responsiveness ensures a reliable and consistent performance suitable for a wide range of applications. These improvements collectively make the proposed haptic device a robust and versatile solution for delivering high-quality haptic feedback.

Haptic gloves	**Power consumption per actuator**	**Maximum blocking force (for whole finger)**	**Cover all finger regions**	**Responsiveness (Activation/Deactivation time)**
Design and development of a 4 dof portable haptic interface with multi-point passive force feedback for the index finger [14]	20 W	2 N	Yes	Activation time 10 ms
Dextres: Wearable haptic feedback for grasping in vr via a thin form-factor electrostatic brake [5]	< 60 mW	20 N	DP-only	Activation time ~50 ms
Dextrems: Increasing dexterity in electrical muscle stimulation by combining it with brakes [54]	< 600 mW	25 N	IP and PP	Activation time 12.5 ms
Glove- and sleeve-format variable-friction electrostatic clutches for kinesthetic haptics [12]	< 3 mW	50 N	DP-only	Activation time < 5 ms Deactivation time > 5 s
This work	**6 mW**	**30 N**	**Yes**	**Activation time < 1s** **Deactivation time < 1s**

Table 2.1: The purposed haptic gloves' performances in comparison with the similar previous works

Chapter 3. Electrostatic Clutch Operating Principal

This section explains the working principle of the ES brake and the basic performance of the force rendered by the proposed configuration. An ES clutch forms a braking mechanism that utilizes the friction between two or more components generated by electrostatic adhesion. Here, the ES clutch mainly consisted of (1) conductive layers, where one is fixed, and the other layer is attached to the sliding components, and 2) dielectric layer (PVDF), a thin insulating layer that separates the electrodes. An electrostatic attraction occurs between the conductive layers if a relatively high voltage is applied (>300 V) to one conductive layer.

As shown in Figure 3.1, a brake is formed that provides passive force feedback by engaging or disengaging the clutch module via electrostatic adhesion. To engage, voltage is applied to create jamming between layers, which resists the motion of the sliding mechanism (Figure 3.1b). On the contrary, applying 0 V will disengage layers to slide over each other freely (Figure 3.1a). Recent haptic gloves [5, 12] have adopted the same approach, but they focused on rendering force feedback on a single point of a finger which is not sufficient for full object perception upon grasp. Also, these works utilized a single side of electrodes to create braking force, which would require a large footprint to install the braking module.

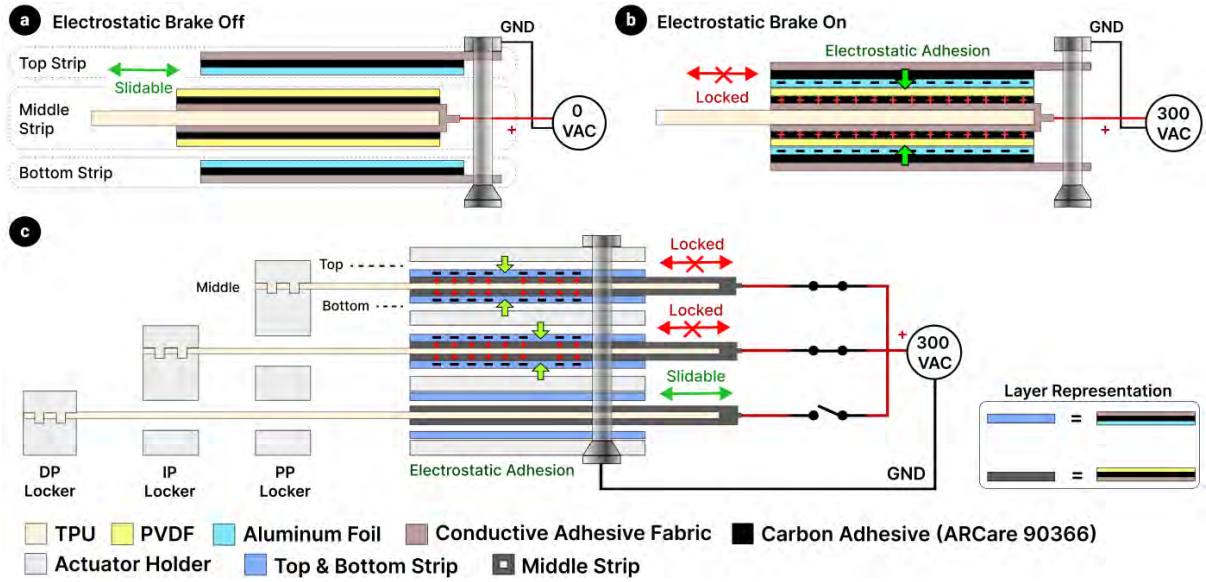

Figure 3.1: Operating principle of ES clutch used in the haptic glove. (a) Top and bottom strips freely slide over the middle strip when there is no difference of electrical potential (0 V). (b) When the voltage (>300 V) is applied, electrostatic adhesion occurs to lock between layers. (c) Multiple ES brakes to provide force feedback to each phalanx.

This work proposes a double-layer structure for the ES clutch to maximize the overlap area, leading to higher force per unit area efficiency. The module consists of 3 flexible strips that do not interfere with finger movement. The top and bottom strips work as conductive layers. They are electrically connected and fixed on the back of the hand. The middle strip consists of conductive materials on top and bottom and a thin dielectric layer coated on top of both surfaces. The middle strip from each module

is connected to the designated phalanx to transfer the force when braking occurs. The top and bottom strips face toward the dielectric layer of the middle strip to impose voltage through electrodes creating the electric charges to accumulate on the surface. Once enough charges are accumulated, electrostatic adhesion occurs to lock the sliding movement of the middle strip connected to each phalanx. Eventually, the movement of the finger is blocked by the braking force exerted upon activation. On the other hand, the phalanx freely slides upon deactivation with applying 0 V.

The theoretical background of the braking mechanism is described below.

$$F_{friction} = \mu F_{attraction} \tag{3.1}$$

$$F_{attraction} = \frac{\varepsilon_0 \varepsilon_r A V^2}{2d^2} \tag{3.2}$$

Equation 3.1 shows the calculation of a total friction force ($F_{friction}$), and μ denotes the friction coefficient. Equation 3.2 is derived from Coulomb's law where ε_0 is the permittivity of vacuum, which has a value of about 8.854 $\times$ 10^{-12} F/m, ε_r refers the relative permittivity (dielectric constant) of the dielectric film between the electrode, A denotes the overlap area between middle strip and other strips, d is the distance between a middle strip to either top or bottom strip (dielectric film thickness), and V is the potential difference between top-middle and bottom-middle strips. Friction force ($F_{attraction}$) refers to the force that blocks the movement of each phalanx.

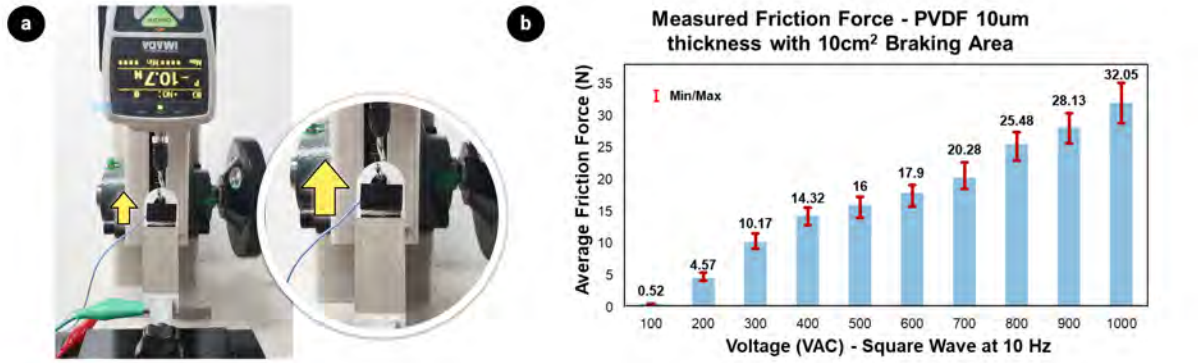

Figure 3.2: Friction force measured for applied voltage between 100 V and 1000 V. The initial overlap area was 10cm^2 and the pulling speed was around 0.5 mm/s.

The ES clutch module is fabricated using PVDF film (β-phase uniaxial orientation, PolyK) with a dielectric constant of 12 and an overlap area of 10 cm^2. Due to the presence of space charges [7,61] that accumulate over time with the dielectric region and lower the attraction force, AC is preferred over DC as the switching of polarity can prevent the accumulation of space charges.

$$P = \frac{E}{t} = \frac{fCV^2}{2} = \frac{f\varepsilon_0 \varepsilon_r A V^2}{2d} \tag{3.3}$$

Equation 3.3 shows the power required (P) to operate the ES brake where E is the energy to charge the clutch per time (t), f is the frequency, C is a variable capacitor formed by the layer structure, and V is the applied voltage between strips. To minimize the space charge and power consumption, a switching frequency of 10 Hz is chosen since the lower frequency is not fast enough to mitigate space charge. From equation 3.3, the required power and current can be calculated under 300 VAC with 10 Hz bipolar square wave, and the dielectric film's properties are k = 12, d = 8 μm, and area = 10 cm^2. The

power consumption for each brake activation is 5.976 mW. While the single LRA has voltage and current consumption of 0.3 VAC and 12.4 mA, respectively.

The relationship between braking force at different voltage levels under the overlap area of 10 cm^2 with a dielectric thickness of 10 μm is shown in Figure 3.2. Friction force appeared at 200 V and increased proportionally to the increased voltage. According to the design guidelines for developing a safe electrical system with the human body [62], the current threshold to start sensation is around 1 mA. While voltage, which might not be the main cause of danger as current, the stimulus can be perceived when the level is over 330 V [63]. Therefore, the operating voltage of 300 VAC was chosen, and the current was limited below 100 µA, which is within the safe range.

Chapter 4. System Overview

Building a robust electrostatic haptic glove system presents several challenges. First, the material choice for creating actuation is critical, as its properties directly affect the quantity of force feedback. Here, the focus was on selecting the material to ensure a balance between the quantity of generated force, durability, and release time (upon deactivation). Subsequently, attention was directed towards building a self-contained system containing a high-voltage power supply from the battery and a high-voltage power controller capable of handling up to eight ES brakes. Lastly, user comfort is maintained by minimizing glove weight and designing mounting structures to avoid finger motion interference.

4.1 Fabrication of Multi-Phalanx ES Brake

Dielectric Material Selection The dielectric material is a core element that determines the performance of the ES brake. The dielectric constant and the thickness of the dielectric material are directly proportional to the electroadhesion force amplitude and required power consumption as shown in Equation 3.2 & 3.3. However, due to durability and safety concerns, a thin dielectric layer cannot be simply used. In terms of durability, frequent activation of the ES brake would incur worn-out on the dielectric layer and lead to short circuit damage. For safety, selected dielectric material should withstand the breakdown upon imposed voltage.

Early ES clutch work [8] used high dielectric material like a fluoropolymer embedded with barium titanate (Luxprint, Dupont) for ES clutches. Due to its brittle characteristics, however, Luxprint is not appropriate for the prototype requiring high flexibility. Although other work suggested using Kapton and PET tape [5] with ductility and high mechanical strength, dielectric constants are relatively low. To this end, researchers started to employ vinylidene fluoride-based polymers such as PVDF (k=12, E=>2000 MPa), PVDF-HFP (k=10, E=1500 MPa), and P(VDF-TrFE-CTFE) (k=40∼50, E=150 MPa) since they showed high flexibility and a relatively high dielectric constant. Recent works used P(VDF-TrFE-CTFE) since it showed the highest dielectric constant with the lowest Young's modulus [15, 56]. However, the softness of P(VDF-TrFE-CTFE) led to stickiness and a prolonged release time (>5 s) after deactivation. This work selected PVDF as the dielectric material, which exhibits the balanced properties between softness and dielectric constant to support flexibility while minimizing the release time (>1 s).

ES Brake Structure As shown in Figure 4.1a, the proposed ES clutch for activating a single phalanx consists of top & bottom strips with aluminum electrodes and one sliding strip in the middle. Figure 4.1b illustrates the ES brake components. For top & bottom strips, the 100 μm thick conductive fabric (ID-NRA01, DImaterials) with 15 μm aluminum foil was layered using 33 μm thick double-sided carbon adhesive (ARCare 90366, Adhesive Research). With this layer structure, capacitance was increased, surface roughness was reduced, and air holes from the conductive fabric were filled to prevent sparking. Then, a T-shape pattern was laser-cut to fit into the actuator holder. These strips were made with dimensions of 5 cm length and 1 cm width, forming an overlap area of 10 cm^2 when configured as a double layer. The overall ES brake comprises 8 ES clutches connected to phalanges (3 phalanges for the index and middle fingers and 2 phalanges for the thumb). Holes were made in the T-shape pattern to secure the top and bottom strips while maintaining electrical connections through the steel bolt.

For the middle strip (sliding strip), 400 μm thermoplastic polyurethane (TPU) with a width of

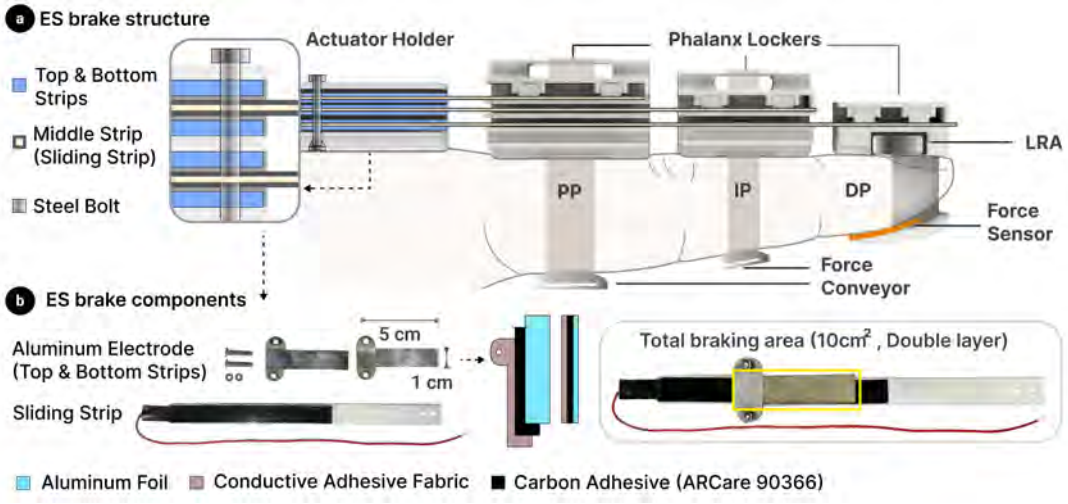

Figure 4.1: ES brake structure and components. (a) ES brakes are connected to all phalanges. (b) A single ES brake includes two aluminum electrode strips and a sliding strip to form an overlap area of 10 cm^2.

1.4 cm was used. The strip's length covers from the actuator holder to the designated phalanx, ensuring a consistent overlap area regardless of the bending of the phalanges. Two holes were made at the end of this strip to assemble with the phalanx locker. On top of the TPU base, 110 μm thick double-sided adhesive tape (468MP, 3M) was attached, followed by laser-cut conductive fabric with a width of 1.2 cm. A 0.1 cm gap was left from the edge to prevent unexpected short circuits. Then, the 10 μm thick PVDF film was placed using carbon adhesive with a width of 1.4 cm to fully cover the conductive fabric. Careful processing of this fabrication was carried out to prevent any wrinkles or air bubbles that may deteriorate performance and lifetime. Lastly, wires were connected at the tip of each strip and wrapped with insulation tape.

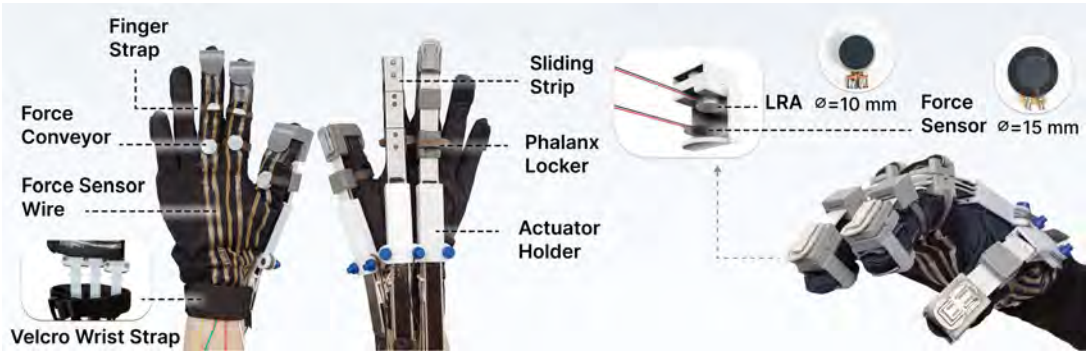

Figure 4.2: Overview of haptic glove prototype and components.

Proof-of-concept Haptic Glove As depicted in Figure 4.2, a proof-of-concept haptic glove comprises 3 actuator holders. These holders are attached to the glove using Velcro, with a Velcro wrist strap also affixed to the actuator holder to secure the prototype. The ES brake is configured by stacking ES clutches in the order of DP, IP, and PP (Figure 4.1a) to transfer blocking force to each phalanx individually. Phalanx lockers were 3D printed using polylactic acid (PLA), connecting to the sliding strip. Clutch passages were formed inside the PP and IP phalanx lockers to allow the sliding of DP and IP strips,

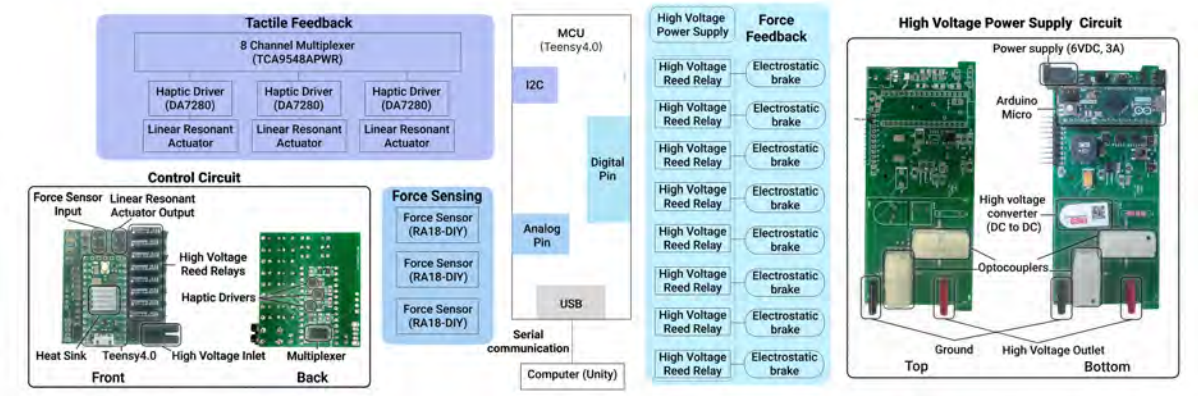

Figure 4.3: Multi-phalanx ES brake system flow. ES brakes and LRAs are employed to create force and tactile sensation. The control circuit and portable high-voltage supply enabled force feedback sensation on multiple phalanges.

while also preventing potential buckling of the strips during finger bending. For IP and PP, the phalanx lockers were wrapped with fabric straps clipped with a TPU force conveyor to intensify force perception. Regarding DP, the phalanx locker covers the whole fingertip to transfer tactile sensation, with added linear resonant actuators (VG1040003D, Vybronics). The focus was primarily on supporting the thumb, index, and middle fingers, as increasing the number of fingers does not improve the perception of the virtual objects' shape [23, 64].

A force sensor (RA18-DIY, Maveldex) was added to the fingertip to prevent engaging braking force beyond the system limit to measure the force applied to the fingertip when the ES brake activates. This setup allows the system to detect instances when a user releases the object or applies too much force. Force sensors were wired with laser-cut stretchable conductive fabric (Technik-tex P130, Shieldex) using heat adhesive (Bemis), as shown in Figure 4.2.

4.2 Hardware Implementation

A customized control circuit was designed as illustrated in Figure 4.3. A Teensy 4.0 microcontroller (600MHz ARM Cortex-M7) was utilized, with digital pins connected to high-voltage reed relays (131-1-A-3/1D, Pickering Electronics) to regulate the ES brakes' on/off state. Additionally, a multiplexer (TCA9548A, Texas Instruments) with a motor driver (DA7280, Renesas Electronics) was employed to actuate multiple LRAs. The overall dimension of the control circuit was 45 cm × 50 cm, which is small enough to be mounted on the arm. To create a battery-powered portable high voltage supply (>300 V), a modification was made to a previous work [65] to further generate bipolar square wave signals from 6 VDC. Two additional optocouplers and MOSFETs were added to form an H-bridge, and the extra MOSFET was driven with the inverse signal from the output of the original MOSFET. The total weight of the gloves comes out as 180 grams (130 grams for the gloves and 50 grams for the control circuit). The ES brake weighs only 10 grams per phalanx.

Chapter 5. Technical Evaluation

Technical evaluations were conducted to confirm the performance of the ES brake. Durability was explored by testing the activation cycle, and force feedback capability was assessed by measuring the force transferred to each phalanx.

5.0.1 Fatigue Life

For this evaluation, the ES brake was repeatedly activated, and a load was applied until the electrodes slipped from each other, reaching the maximum braking force. This allowed for the measurement of the realistic fatigue life of the proposed ES brake. The same setup was used to measure the friction force (Figure 3.2), where the sliding strip was connected to a push-pull gauge (ZTA-200N, Imada), while another electrode was fixed to its base. During testing, 10 μm thick PVDF was used with an operating voltage of 300 VAC at 10 Hz, with an overlapped area of 10 cm^2, supporting an average braking force of 10.17 N. Throughout 600 trials, the observed force ranged from 8.4 N to 11.5 N, with no significant decrease in the braking force noted.

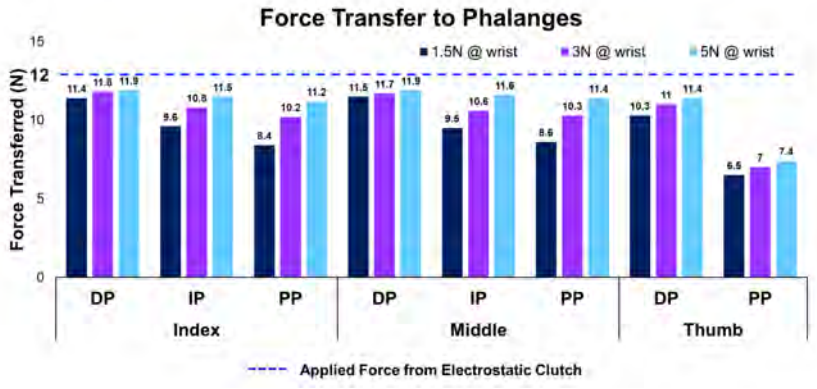

Figure 5.1: ES brake transferred force to each phalanx for 3 different wrist anchoring forces (1.5 N, 3 N, and 5 N). ES brake provided a maximum of 12 N (350 VAC with 10 Hz and an overlap area of 10 cm^2.

5.0.2 Force Feedback Validation

Since the ultimate goal is to provide braking force to each phalanx for grasp, it is critical to assess how much force is actually transferred to each phalanx with the prototype. To measure the normal forces acting on the phalanx, the calibrated force sensors-RA18-DIY were installed for testing purposes. Force sensors were also added to the wrist strips to explore the relationship between anchoring force and transferred force. For the evaluation, the braking force of 12 N was activated for each phalanx, and users were instructed to perform a full grasp to obtain the maximum transferred forces.

Figure 5.1 illustrates the results of the evaluation. On average, force transfer rates of 95%, 80%, and 70% were observed on DP, IP, and PP for index and middle fingers when anchored on the wrist with 1.5 N. With the increase in wrist anchoring force from 1.5 N to 5 N, a high increase in force transfer rates (more than 90% on average) was detected. The DP exhibited a high force transfer rate because the

phalanx locker covers the whole fingertip with the rigid body. On the other side, IP and PP showed less force transfer since the force was transferred through flexible TPU. For the thumb, PP has a significantly lower force transfer rate. This is possibly due to the anchoring point of the thumb's PP being located around the Carpometacarpal joint (CMC), which naturally moves along the motion of the thumb's PP.

Chapter 6. Haptic Rendering with Electrostatic Brake Haptic Glove

Previously, the force feedback on different phalange has been suggested [45]. However, users' capability to distinguish the applied forces at different phalanges and how users perceive the blocking forces at multiple phalanges have not been fully explored. To address this gap, an exploratory study was carried out to find out two key aspects of human force perception on the finger: (1) the accuracy of force localization across different phalanges and (2) the perceived force patterns when blocking forces presented at multiple phalanges. The findings from the study were utilized to form ES brake actuation conditions to provide effective and efficient force feedback.

6.0.1 Exploratory Study

The exploratory study had two main sessions. In the first session, users identified the perceived location of the braking force during the grasp. The prototype activates an ES brake on a single phalanx location. The possible phalanx locations include the Distal Phalanx, Intermediate Phalanx, and Proximal Phalanx of the index, middle, and thumb, as shown in Figure 6.1a. Then, participants identified the perceived location of the phalanx. Users carried out a total of 24 trials (8 locations $\times$ 3 set).

In the second session, a study was conducted to investigate how users perceived the force across the finger segments for different combinations of multi-phalanx force feedback. A total of 14 different combinations of multi-phalanx force feedback patterns were utilized as shown in Figure 6.1b. DP dominant tasks and PP dominant tasks were configured, where constant braking force was supported to DP or PP while activating braking force in various patterns. Additionally, cases with braking force activated on all phalanges for each finger were included. Participants completed a total of 42 trials (14 patterns $\times$ 3 set). The entire study lasted about 40 minutes.

16 participants (9 women and 7 men; Mean=26 years old, SD=4.1) were recruited and asked to wear a haptic glove on their dominant hand. They were fully instructed about the user study and consented before the study. The device was operated at 350 VAC at 10 Hz, creating a maximum of 12 N braking force. Before conducting the test, all phalanges were activated individually to familiarize participants with the sensation of force from the device. During the study, participants were blindfolded to remove bias caused by visual information from the sliding strip movement. They were then asked to bend their hands slowly and verbally indicate which phalanx was being blocked.

Results and Discussions

The participants demonstrated an overall perception accuracy of 74% in detecting the location of the phalanx with applied braking force (Figure 6.1a). As expected, the DP of the index and middle fingers showed the highest accuracy within a finger due to DP's high sensitivity [66]. Conversely, the PP was better localized on the thumb, likely due to the structure of the carpometacarpal (CMC) joint, which caused larger PP movements when bending the DP compared to the index and middle fingers. The IP had the lowest accuracy in the index and middle fingers, as participants often misinterpreted sensations on the IP as those on the PP. This is likely due to the hierarchical finger bone structure, where blocking the IP also restricts movement in the PP.

In the second session, the investigation found that users accurately identified certain multi-phalanx

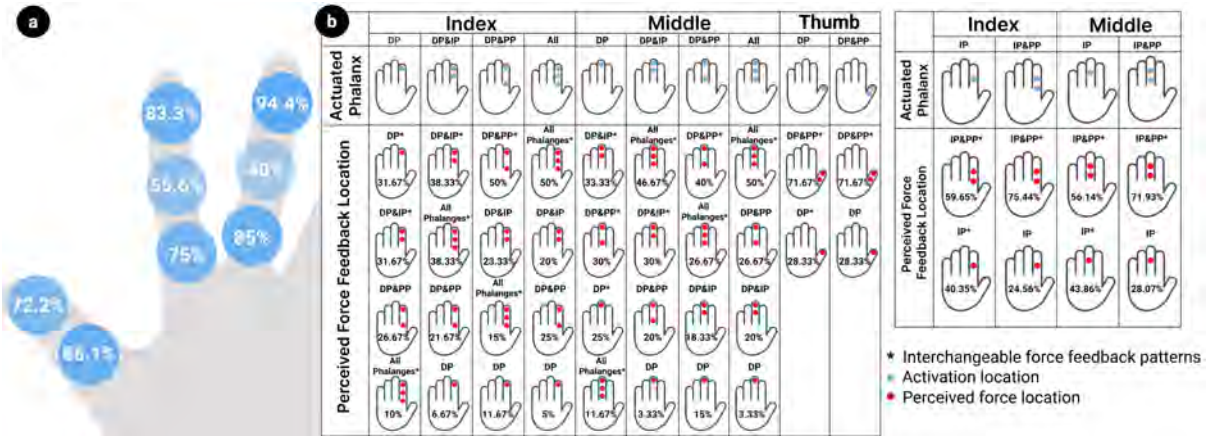

Figure 6.1: The result of an exploratory study on force localization perception accuracy with the proposed device. (a) Identification accuracy when a single braking point is applied at a single phalanx, (b) Perceived force feedback location distribution when multiple braking points are applied at multiple phalanges.

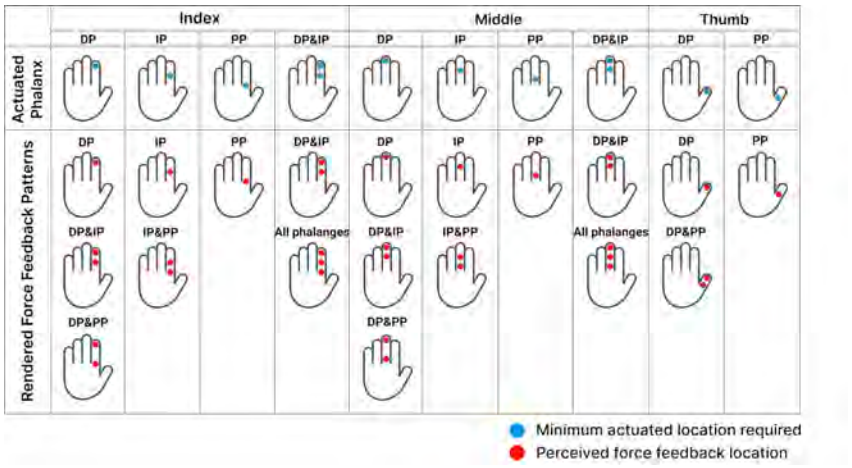

Figure 6.2: Designated haptic rendering patterns for applying ES brake(s) (blue dots) to stimulate various force feedback patterns (red dots).

force feedback patterns such as DP-only or DP&IP. However, a common error was generally observed when providing braking force to the adjacent phalanx, mainly due to characteristics of hierarchical bone structure. For example, providing a force on DP created a sensation on DP as well as DP & IP. For the thumb, 71.7% of participants reported the sensation of the force feedback on 'DP & PP' regardless of applied braking force patterns.

From these results, interchangeable force feedback patterns were drawn, as illustrated in Figure 6.1b. The study revealed that activating fewer ES brakes could elicit a similar sensation compared to activating all the intended phalanges.

6.0.2 Haptic Rendering Algorithm

To formulate power-efficient rendering while maintaining performance, a data-driven approach for haptic rendering was employed. Rather than activating every phalanx in contact with a virtual object,

insights from the exploratory study were leveraged to identify a minimal set of ES brakes to activate while maintaining similar perceived force patterns for the user (Figure 6.2). If the user's perception of force with a minimal set of activated brakes closely resembled the perception with a larger set, these patterns were grouped together. The blue dots in Figure 6.2 represent the efficient rendering pattern, which can effectively render the red dot patterns in the same column. For example, if collision detection occurs at the index DP and IP phalanges, the algorithm would only activate the ES brake on the DP. This is because the user's perception of force with activating the ES brake for the DP was similar to activating the ES brakes for DP&IP.

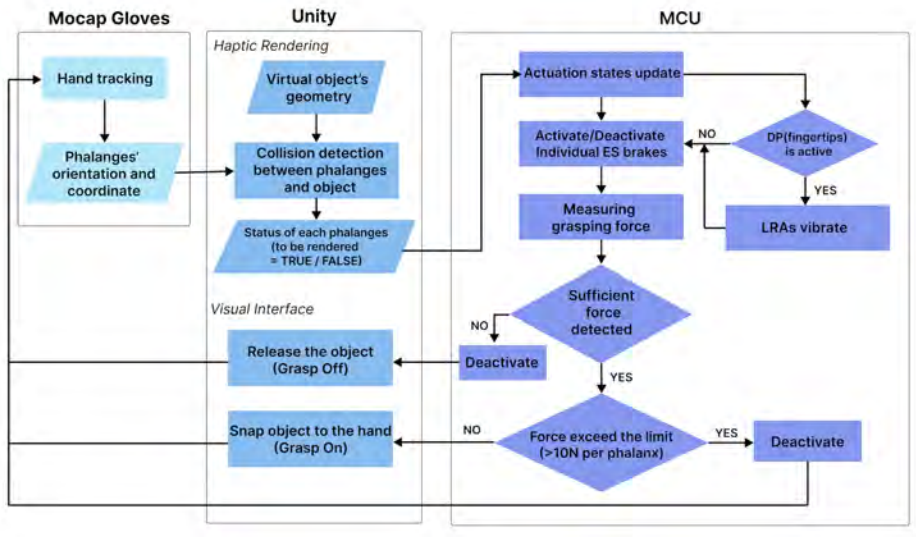

Figure 6.3: Haptic rendering pipeline. Haptic rendering patterns from the exploratory study were employed to support force feedback on multiple phalanges for the index, middle, and thumb.

Figure 6.3 illustrates the overall haptic rendering pipeline. Haptic feedback was rendered based on the collision detection between virtual objects and the phalanges during grasping interactions. Hand-tracking data was obtained from the motion capture gloves module (Quantum Gloves, Manus Meta), which was mounted on top of the prototype. Whenever the virtual phalanges were in contact or out of contact, the changes in the status of that phalanx were sent to the MCU. Based on the haptic rendering patterns set in Figure 6.3, the system determined activation of ES brakes accordingly (Actuation states update in Figure 6.3).

For the tactile feedback, the LRAs vibrated when the DP state changed from inactive to active state. Using the force sensor attached to each fingertip, the physical status of the applied force on the user was monitored. Based on the force measurement, the virtual object was either snapped or released from the hand. Force measurements were also monitored to prevent damage to the ES brake by disengaging it when the applied force was too high (>10 N).

Chapter 7. User Study

In the user study, the quantitative and qualitative object perception performance of the proposed device was compared to the conventional single-point (DP) force feedback approach. The hypothesis is that by stimulating multiple finger segments would provide more accurate haptic cues for shape recognition. For quantitative feedback, the identification accuracy of different finger phalanx-angle positions was evaluated. In terms of qualitative assessment, user experience during interaction with various object shapes was examined. To comprehensively evaluate these aspects, two user studies were conducted. First, the capability to perceive different levels of phalanx-angle positions was tested. Then, user experience with various object shapes was assessed using this approach and other baselines. These studies verified the effectiveness of the proposed multi-phalanx ES brake for shape perception and provided valuable insights into the user experience associated with this approach.

7.0.1 User Study 1: Phalanx-Angle Position Perception

In User Study 1, the performance of supporting multi-phalanx force feedback was evaluated by validating the number of bending levels perceivable through multi-phalanx force feedback. A within-subject study aimed at determining the perceivable angle resolution was carried out. The tasks required participants to bend their hands around different joints, which mimicked grasping objects with various shapes and angles. The multi-phalanx approach was compared to a single-point method, with results indicating that the multi-phalanx approach was superior in distinguishing various levels of angles with greater accuracy.

Study Setup 17 participants (7 women and 10 men; Mean=26 years old, SD=4.43) were recruited. All participants were right-handed and did not have a problem with wearing the prototype. The overall study took about 2 hours. Participants were equipped with white-noise playing headphones and blindfolds to prevent bias from auditory or visual cues.

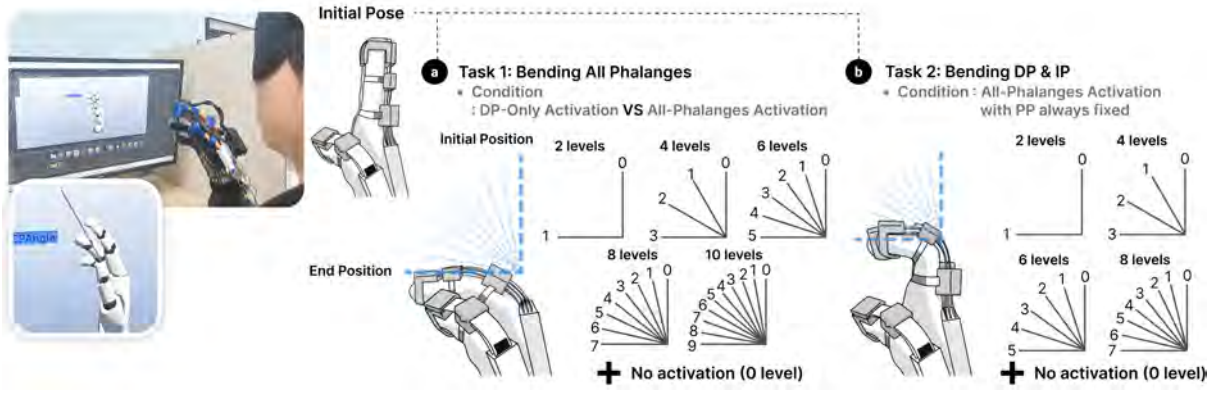

Figure 7.1: Finger phalanx-angle positions perception test study setup. (a) Bending all phalanges together for 5 different levels (2, 4, 6, 8, 10 levels) and (b) bending DP & IP together, while PP was fixed for 4 different levels (2, 4, 6, 8 levels). Both (a) and (b) contained no activation condition as well (0 level).

In this study, participants carried out two tasks as shown in Figure 7.1. First, all-phalanges bending

task (Task 1) and 'DP & IP' phalanges bending task (Task 2). For Task 1, participants were asked to bend the entire phalanges of the index and middle fingers around the metacarpophalangeal (MCP) joints. For Task 2, participants were instructed to bend their DP and IP around the proximal interphalangeal (PIP) joints while keeping the PP fixed. The wrist position was fixed as a pivot point in the virtual scene. The ES brake was activated when the position of the phalanx reached a certain degree of angle, which was randomized for the trials.

Task 1 involved five stages with different angular resolutions. The angle of 90 degrees were divided into 2, 4, 6, 8, and 10 levels for each stage, with the degrees between each level being 90°, 30°, 18°, 11.3°, and 10°, respectively. Task 2 comprised 4 stages, dividing 90 degrees into 2, 4, 6, and 8 levels. A 'No Activation' case (0 level) was included in both tasks where no force feedback was provided to the fingers. A study on DP bending with the fixation of IP and PP was not conducted due to the limited adduction and abduction movement range, which was below 40° [67], rendering it insufficient for meaningful angle divisions for force feedback.

For Task 1, two activation conditions were provided (DP-only vs. all-phalanges activations), and the results were compared. In Task 2, only all-phalanges activation conditions were conducted. All stages were repeated twice, except for the first stage discriminating 2 levels, which was repeated 3 times to obtain an equivalent number of data points to other level conditions. Figure 7.1 illustrates the overall design of User Study 1.

Study Procedure A walkthrough session was conducted where participants went through all conditions to become acquainted with the system and reference cues. Then, participants were asked to slowly flex all phalanges around their MCP joints (Task 1) or bend the DP&IP phalanges around PIP joints (Task 2). All conditions were randomized and counterbalanced. Participants verbally responded at which level they felt the blocking force, with a response of 0 level if they did not feel any force. After repeating each stage twice, the next stage was proceeded to. For Task 1, two activation conditions were tested, including DP-only and all-phalanges activation. A 10-minute break was provided between Task 1 and Task 2. A total of 94 trials were conducted (70 trials for Task 1 with 2 activation conditions, 24 trials for Task 2), yielding 3246 responses (94 trials × 17 participants × 2 repetitions).

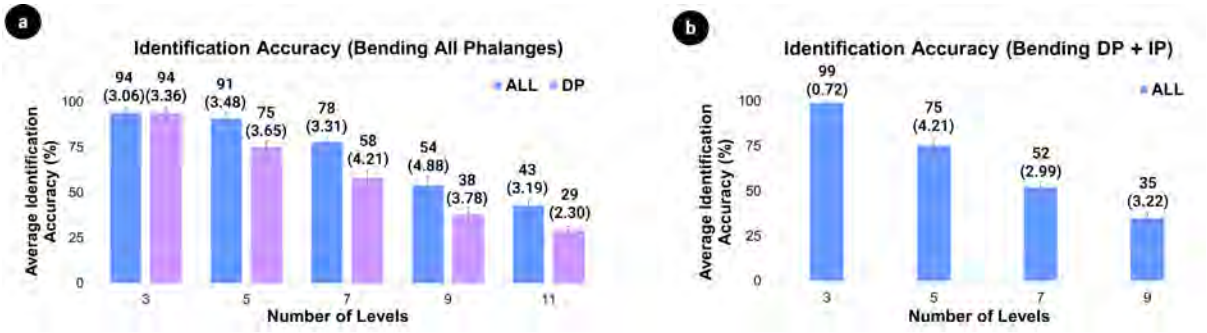

Figure 7.2: The average identification accuracy of the phalanx-angle positions perception test. (a) The comparison of identification accuracy between all-phalanges and DP-only activation conditions when all phalanges are bending together and (b) the identification accuracy of all-phalanges activation condition when bending DP and IP while PP is fixed. The error bars represent standard errors.

Results The objective of the study was to investigate supportable angle resolution with the device and compare the performance of braking all phalanges against the conventional DP-only approach. For Task 1, accuracy rates were averaged across all levels within each stage, thereby obtaining the

accuracy rate for each stage. Furthermore, the accuracy rates of the same stages were compared between two activation conditions: DP-only activation (DPA) and all-phalanges activation (APA), as shown in Figure 7.2a.

Overall, results showed that DPA has a steeper decline in accuracy as the number of levels increased. On the contrary, APA maintained a relatively high accuracy where it showed >90% accuracy for identifying 5 different levels of bending angles. Still, a significant drop in performance was observed across all conditions when the number of levels increased to 7 or above. Therefore, it was confirmed that the device supports a clear sensation of angle resolution of 18° for most users and showed superior performance compared to DPA. For Task 2, it was found that the device supports rendering an angle resolution of 30° when bending around the PIP joint, which was lower than when bending around the MCP joint.

In this study, it was confirmed that the approach of utilizing all phalanges for force feedback superseded existing DP-only force feedback. The assumption is that stabilizing the position of a finger appropriately using the APA condition contributed to better performance. A decrease in identification accuracy was also observed when a finger was bent more. This decrease is assumed to be due to the nature of using a soft fabric as a base structure, where the elongation of the fabric before activating the ES brake reduced the amount of braking force.

7.0.2 User Study 2: Object Perception Experience

In Study 2, the overall experience of using the proposed device while grasping four different virtual objects was evaluated. The subjective ratings of three ES brake activation strategies, including DP-only, all-phalanges, and all-phalanges with the haptic rendering pipeline, were compared. Activating ES brakes using this approach showed a relatively better experience. Qualitative user feedback was obtained to address the limitations for future development.

Study Setup The study was conducted with the 16 participants from Study 1, utilizing a within-subject design experiment where all participants explored identical objects for three different conditions. The overall study took about 30 minutes. Participants were guided to watch a monitor displaying VR scenes where virtual hands interacted with virtual objects. Additionally, 3D-printed physical objects with the same geometry as the testing virtual objects were provided, allowing users to refer to these objects as the ground truth reference.

Four objects with various shapes, such as a sphere, quadrangular prism, triangular prism, and cylinder, were provided. Three haptic feedback rendering conditions were implemented, including DP-only activation as a baseline, all-phalanges activation, and all-phalanges with the rendering approach (Adaptive activation), utilizing the rendering pipeline from Figure 6.3. For this test, the virtual hand position was fixed, and users were only allowed to perform grasping actions. This approach allowed for a focused evaluation of the grasping motion. Figure 7.3 illustrates the overall sequence of Study 2.

Participants were asked to provide subjective ratings of 3 conditions by answering 5 questions related to 5 haptic experience keywords [68] (Realism: *How realistic was the feeling of the object?* , Comfort: *How comfortable was the interaction?* , Immersion: *How does haptic feedback increase your involvement in grasping?* , Harmony: *How appropriate is the haptic feedback on where and when you felt it?* , and Satisfaction: *How do you like having haptic feedback as part of your experience?*). Participants rated using a 7-point Likert scale ranging from 1 to 7 through the online form via tablet.

Study Procedure Before getting any haptic feedback, participants were instructed to grasp reference physical objects so they could refer to these grasping sensations as ground truth experiences. Then,

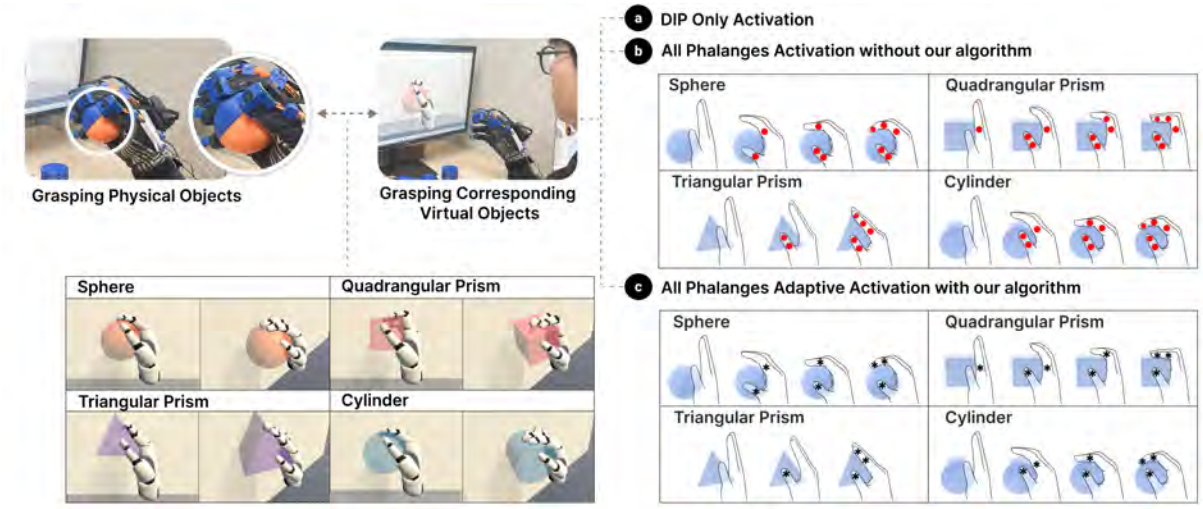

Figure 7.3: Object perception study with sphere, quadrangular prism, triangular prism, and cylinder using 3 haptic feedback conditions including (a) DP-only activation, (b) all-phalanges activation, and (c) all-phalanges with adaptive activation.

participants were asked to bend their fingers and grasp the virtual object. Virtual objects were presented in randomized order. For the presented object, all activation conditions were given in a random order without disclosing condition information. Participants were guided to thoroughly explore each condition's sensation until they felt confident enough to respond to the questionnaire. A total of 960 data points were collected (4 objects $\times$ 3 haptic rendering conditions $\times$ 5 questions $\times$ 16 participants). Following the study, a brief interview session was conducted to gather feedback on the overall experience of interacting with virtual objects under the given force feedback conditions.

Results To assess the impact of haptic activation conditions on each keyword across different objects, the Wilcoxon signed-rank test was applied for analysis, as depicted in Figure 7.4. Since there is no significant difference between all-phalanges adaptive (ADA) and all-phalanges condition (APA), thus it was only compared with the DP-only activation (DPA) condition. A significant enhancement was noticed in the overall experiences with the quadrangular and triangular prism but a relatively small enhancement in realism and satisfaction with the sphere and cylinder.

Significant differences were observed across various keywords. For realism, distinctions were found between DPA and APA conditions for the quadrangular prism ($p = .026 < 0.05$), triangular prism ($p = .031 < 0.05$), and cylinder ($p = .04 < 0.05$), as well as between DPA and ADA conditions for the sphere ($p = .021 < 0.05$) and triangular prism ($p = .003 < 0.005$). Comfort ratings displayed significant differences, particularly with the triangular prism, between the DPA and both APA ($p = .04 < 0.05$) and ADA conditions ($p = .026 < 0.05$). Also, the subjective rating of comfort for the sphere with APA and ADA conditions was found to be lower than with the DPA condition. Immersion showed statistically significant distinctions between the DPA and APA conditions for the quadrangular ($p = .003 < 0.005$) and triangular prism ($p = .026 < 0.05$), and between DPA and ADA conditions for the triangular prism ($p = .007 < 0.05$). Harmony ratings exhibited significant differences between the DPA and APA conditions with the quadrangular prism ($p = .005 < 0.05$), and between DPA and ADA conditions for both quadrangular ($p = .021 < 0.05$) and triangular prisms ($p = .005 < 0.05$). Lastly, satisfaction ratings differed significantly between the DPA and APA conditions across all objects, including the sphere ($p = .022 < 0.05$), quadrangular prism ($p = .01 < 0.05$), triangular prism ($p = .032 < 0.05$), and

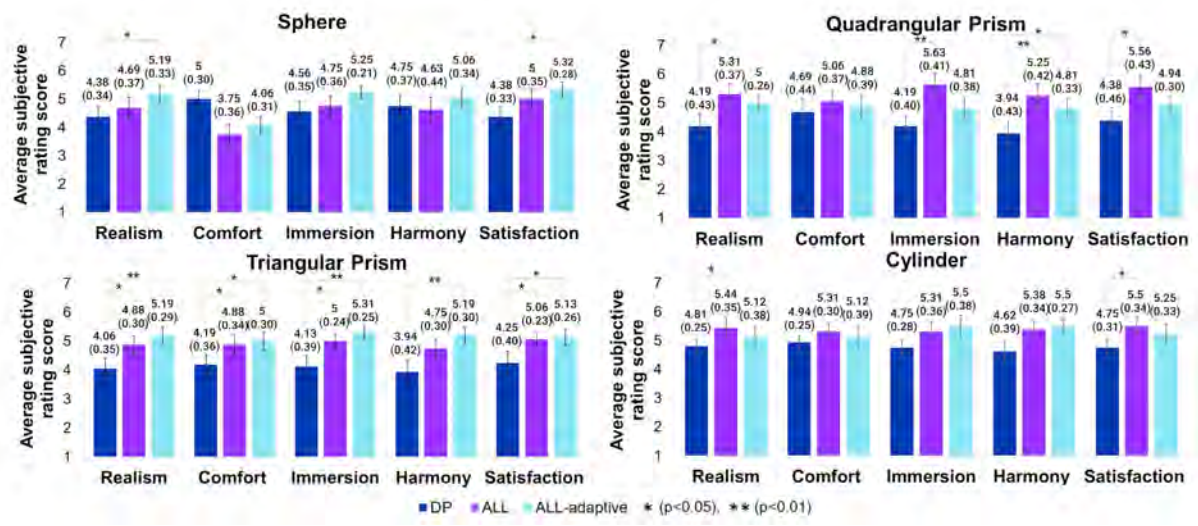

Figure 7.4: The object perception experience ratings for various haptic feedback conditions. Each bar graph refers to the subjective rating from the participant under five criteria including realism, comfort, immersion, harmony, and satisfaction.

cylinder ($p = .031 < 0.05$), with additional notable differences between the DPA condition and ADA condition for the triangular prism ($p = .032 < 0.05$).

The activation of all phalanges showed better object perception experiences than only activating DP across most haptic experience keywords. Using all-phalanges activation, users could maintain postures required by different shapes of objects. For example, a triangular prism required participants' hands and fingers to be straight and flat, and a quadrangular prism required a 90° edge shape by providing the blocking sensation on the phalanges around MCP joints. In contrast, objects with rounded shapes like spheres and cylinders did not require the exact representation of edges, which can be easily rendered with DPA condition. This explains the reason why there was no significant difference across overall keywords for sphere and cylinder.

Qualitative Feedback Feedback from 5 participants highlighted that the quadrangular and triangular prisms provided the most realistic sensation of grasping. This is probably because multi-phalanx sensations were emphasized with these objects compared to rounded shapes. Additionally, participants noted that the sensation of manipulating the thumb felt weaker compared to other fingers, which may be attributed to the thumb's limited range of movement, consistent across different objects.

Chapter 8. Applications

The proposed device delivers multi-phalanx haptic feedback to enhance the immersive experience of interacting with high-resolution virtual objects. Its advanced technical functionality ensures rapid activation times, complemented by excellent wearability attributed to its lightweight structure. Additionally, this system is supported by an efficient haptic rendering algorithm. Therefore, this device has the potential to be utilized in various fields including industrial applications and personal applications. The device offers versatile applications across different contexts including industrial training, remote control, entertainment, and telepresence.

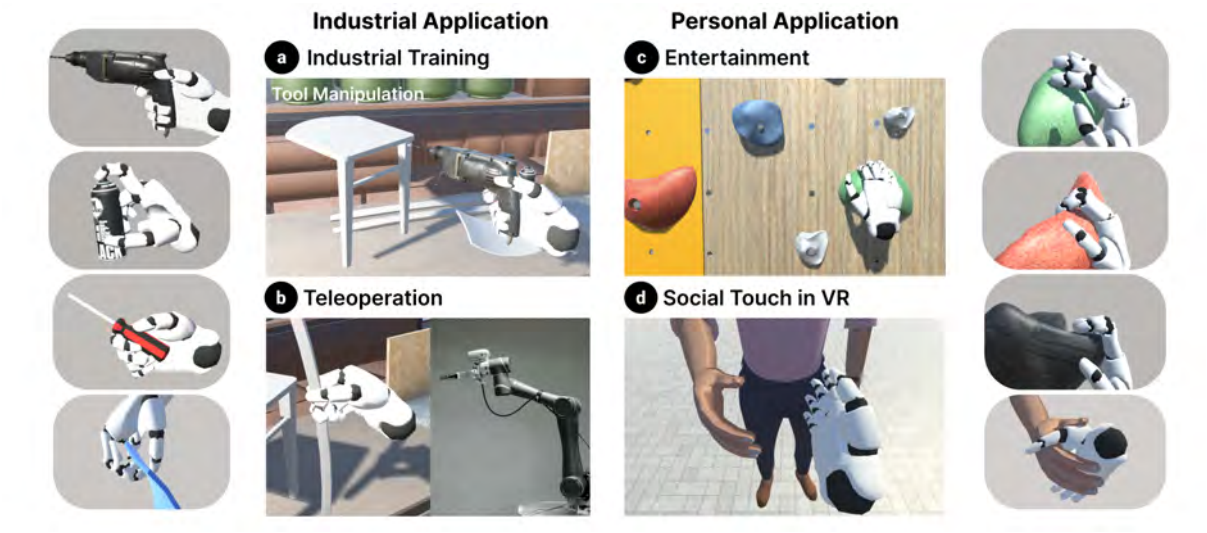

Figure 8.1: Example use case scenarios showing (a),(b) industrial applications and (c),(d) personal application.

Industrial Training Nowadays, industries adopt VR training to reduce the cost and relax the time-space restriction [69]. However, they usually provide a virtual scene without tactile sensation, which plays an important role in tool manipulation or assembly tasks. As the study suggests [70], with the presence of haptic feedback, task learnability has improved, especially for complex assembly tasks. Since the device enables tactile sensation on complex multilateral shapes, it is suitable for VR training scenes that deal with industrial tools. Enabling users to feel like they are actually touching the machinery can closely replicate the actual industrial environment, thereby enabling effective training simulations.

Teleoperation The proposed haptic glove can distinguish the subtle difference between virtual shapes, which can lead to high accuracy performance in teleoperation through VR. Teleoperation via VR is usually executed by moving an object at a distance with the gripper robot while human operators are manipulating the objects in the corresponding virtual scene. Current systems utilize handheld controller devices or bare hands as master controllers and the robot as slave. However, as precisely grasping or manipulating virtual objects is impossible, this device can potentially contribute to improving the performance of teleoperation. By accurately rendering the shape of the object, this glove allows users to have a more secure and nuanced grip on the object. Users can perceive the richer sensation of the size, shape, and texture of the objects, leading to better control over grip strength and end effector

placement. Moreover, relying less on visual cues and more on tactile sensation to understand the object and adjusting the grasp accordingly can reduce the operators' cognitive load [71].

Entertainment VR entertainment contents, including exploring the virtual scene, usually ask users to use controllers to manipulate the virtual objects. However, conventional controllers simply pass through objects without any tactile sensation, which breaks immersion and gives a sense of artificiality. Although there are commercial gloves that provide haptic feedback, they are bulky and inefficient in rendering the object realistically. In particular, games that interact with complex shapes like bouldering, where users touch and grab rocks with multi-edge geometry, require a haptic sensation on intermediate phalanges (IP) and proximal phalanges (PP) as described in Figure 8.1 c. Using the suggested haptic glove, the detailed haptic feedback from the phalanges can provide greater immersion in VR scenes while having a lightweight structure and fast activation time.

Social Touch in VR In a VR scene, socially interacting with other characters is a crucial part of the experience. While there are still limitations to real-like interaction, realism can be enhanced through social touch. Social touch, which is a way of nonverbal communication through gentle physical contact, is a crucial part of human interaction. Experiencing social touch in a VR scene can increase intimacy towards the character and enhance the social telepresence [72]. For users to physically interact with the virtual characters, the device being used needs a haptic feedback functionality. As the device can provide a tactile sensation in the hand, it is suitable for interacting with characters similar to real-life situations.

Chapter 9. Discussion

Several studies have implemented multi-phalanx haptic gloves [14, 45]. Nevertheless, these approaches typically relied on active force feedback mechanisms, resulting in bulky structures and high power consumption. To address these limitations, the ES brake was adopted for its lightweight design (10 grams per brake) and low power consumption. However, challenges arose in dielectric material selection and designing for fast engagement and disengagement. Through multiple design iterations, a balance between critical aspects including wearability (lightweight with comfort), force feedback capability (12 N braking force per phalanx), and manufacturability (low-cost & in-house fabrication process) were achieved.

The user experiments demonstrated significant improvements in phalanx phalanx-angle position perception and user experience (realism & immersion) compared to a baseline with blocking force applied only to the DP. In User Study 1, while the all-phalanges activation condition yielded better performance, the achieved angle resolution of 11.3° exceeded the Just Noticeable Difference of the PIP and MCP joints ($1.7° \sim 2.7°$ when interacting with objects).

User Study 2 revealed similar overall performance between the haptic rendering pipeline (derived from the exploratory study) and the all-phalanges condition (force applied to all phalanges). For objects with multiple edges (e.g., quadrangular prism), a strong and rigid force using all-phalanges condition was preferred, while objects with flat, tilted surfaces (e.g., triangular prism) requiring similar rotation across all phalanges favored the proposed method. Multi-phalanx activation had the least impact on round and curved objects. These findings pointed out that the object's geometry must be taken into account when designing a haptic rendering pattern.

The current design employs an external hand-tracking system. This added 80 grams of weight and introduced potential inaccuracies since this tracking system was originally designed for bare-hand usage. As suggested in prior works [5,12], developing self-sensing capabilities by tracking capacitance changes in three electrode pairs per phalanx could enable more robust hand tracking in the future. Additionally, the current design requires improvement in transferring braking force to the thumb's proximal phalanx (PP) through a mechanism that resists the unwanted Carpometacarpal (CMC) joint movement. To accommodate the feasibility of various grasping postures, the hardware design should be revised to allow greater freedom in abduction and adduction movements.

Lastly, the current control circuit employs high-voltage reed relays, which contain mechanical switches susceptible to wear and tear after prolonged use. Consequently, alternatives for power regulation must be considered to enhance durability and reliability. Solid-state relays (SSRs) might offer a more appropriate solution, balancing fast switching times, superior circuit isolation, and an extended operational lifespan. SSRs eliminate the mechanical wear associated with reed relays, as they rely on MOSFETs and optocouplers for circuit isolation, which operates without physical contacts, thus preventing wear and reducing maintenance as well as safeguarding sensitive control circuits from high-voltage spikes and electrical noise. Furthermore, the rapid switching capability of SSRs can operate in milliseconds, ensuring efficient and precise control. The inclusion of snubber circuits and heat sinks further protects and maintains the relay's performance under varying loads. These advantages make SSRs an ideal option for future control circuit revisions, ensuring reliability and longevity in power regulation.

Chapter 10. Conclusion

This thesis introduces a novel wearable haptic feedback system equipped with multi-phalanx ES brakes. The goal was to improve object shape recognition during virtual reality (VR) grasping. The haptic gloves were designed, fabricated, and evaluated through a user study. In contrast to single-point feedback at the fingers, the study sought to determine whether it would be possible to provide force feedback on several phalanges in order to improve object perception. The results indicated that the suggested approach of multi-phalanx force rendering significantly enhanced realism, immersion, and user satisfaction when interacting with various shapes in VR. This improvement was particularly notable for objects with complex shapes, such as triangles and cubes, where multi-point feedback provided a more accurate representation of the edges and contours of the object. Hopefully, this work will pave the way toward more realistic and immersive VR experiences.

Bibliography

[1] C. W. Borst and A. P. Indugula, "Realistic virtual grasping," in *IEEE Proceedings. VR 2005. Virtual Reality, 2005.* IEEE, 2005, pp. 91–98.

[2] M. Chessa, G. Maiello, L. K. Klein, V. C. Paulun, and F. Solari, "Grasping objects in immersive virtual reality," in *2019 IEEE Conference on Virtual Reality and 3D User Interfaces (VR)*, 2019, pp. 1749–1754.

[3] E. Triantafyllidis, C. Mcgreavy, J. Gu, and Z. Li, "Study of multimodal interfaces and the improvements on teleoperation," *IEEE Access*, vol. 8, pp. 78 213–78 227, 2020.

[4] L. Connelly, Y. Jia, M. L. Toro, M. E. Stoykov, R. V. Kenyon, and D. G. Kamper, "A pneumatic glove and immersive virtual reality environment for hand rehabilitative training after stroke," *IEEE Transactions on Neural Systems and Rehabilitation Engineering*, vol. 18, no. 5, pp. 551–559, 2010.

[5] R. Hinchet, V. Vechev, H. Shea, and O. Hilliges, "Dextres: Wearable haptic feedback for grasping in vr via a thin form-factor electrostatic brake," in *Proceedings of the 31st Annual ACM Symposium on User Interface Software and Technology*, ser. UIST '18. New York, NY, USA: Association for Computing Machinery, 2018, p. 901–912. [Online]. Available: https://doi.org/10.1145/3242587.3242657

[6] T. Nakao, K. Kunze, M. Isogai, S. Shimizu, and Y. S. Pai, "Fingerflex: Shape memory alloy-based actuation on fingers for kinesthetic haptic feedback," *19th International Conference on Mobile and Ubiquitous Multimedia*, 2020.

[7] S. B. Diller, S. H. Collins, and C. Majidi, "The effects of electroadhesive clutch design parameters on performance characteristics," *Journal of Intelligent Material Systems and Structures*, vol. 29, no. 19, pp. 3804–3828, 2018. [Online]. Available: https://doi.org/10.1177/1045389X18799474

[8] S. Diller, C. Majidi, and S. H. Collins, "A lightweight, low-power electroadhesive clutch and spring for exoskeleton actuation," in *2016 IEEE International Conference on Robotics and Automation (ICRA)*, 2016, pp. 682–689.

[9] V. Vechev, R. Hinchet, S. Coros, B. Thomaszewski, and O. Hilliges, "Computational design of active kinesthetic garments," in *Proceedings of the 35th Annual ACM Symposium on User Interface Software and Technology*, 2022, pp. 1–11.

[10] R. Thilakarathna and M. Phlernjai, "Design and development of a lightweight, low-cost cylindrical electrostatic clutch," *Engineering Science and Technology, an International Journal*, vol. 49, p. 101600, 2024.

[11] Q. Xiong, X. Liang, D. Wei, H. Wang, R. Zhu, T. Wang, J. Mao, and H. Wang, "So-eaglove: Vr haptic glove rendering softness sensation with force-tunable electrostatic adhesive brakes," *IEEE Transactions on Robotics*, vol. 38, no. 6, pp. 3450–3462, 2022.

[12] R. J. Hinchet and H. Shea, "Glove- and sleeve-format variable-friction electrostatic clutches for kinesthetic haptics," *Advanced Intelligent Systems*, vol. 4, no. 12, p. 2200174, 2022. [Online]. Available: https://onlinelibrary.wiley.com/doi/abs/10.1002/aisy.202200174

[13] M. Achibet, G. Casiez, and M. Marchai, "Desktopglove: A multi-finger force feedback interface separating degrees of freedom between hands," in *2016 IEEE Symposium on 3D User Interfaces (3DUI)*. IEEE, 2016, pp. 3–12.

[14] M. J. Lelieveld and T. Maeno, "Design and development of a 4 dof portable haptic interface with multi-point passive force feedback for the index finger," in *Proceedings 2006 IEEE International Conference on Robotics and Automation, 2006. ICRA 2006.* IEEE, 2006, pp. 3134–3139.

[15] N. Vanichvoranun and S. H. Yoon, "A lightweight wearable multi-joint force feedback for high definition grasping in vr," in *2023 IEEE Conference on Virtual Reality and 3D User Interfaces Abstracts and Workshops (VRW)*, 2023, pp. 625–626.

[16] R. Ranjithkumar, J. D. Rosario, R. Swaminathan, N. Raju, V. Bhojan, and S. Ayyasamy, "Improved load bearing performance of electroadhesive tapes with hexagonal boron nitride/barium titanate composite in poly (vinylidene fluoride co-hexafluoropropylene)," *Journal of Materials Science: Materials in Electronics*, vol. 34, no. 4, p. 308, 2023. [Online]. Available: https://doi.org/10.1007/s10854-022-09543-5

[17] D. Tsetserukou, S. Hosokawa, and K. Terashima, "Linktouch: A wearable haptic device with five-bar linkage mechanism for presentation of two-dof force feedback at the fingerpad," in *2014 IEEE Haptics Symposium (HAPTICS)*, 2014, pp. 307–312.

[18] F. Chinello, M. Malvezzi, C. Pacchierotti, and D. Prattichizzo, "Design and development of a 3rrs wearable fingertip cutaneous device," in *2015 IEEE International Conference on Advanced Intelligent Mechatronics (AIM)*, 2015, pp. 293–298.

[19] M. Gabardi, M. Solazzi, D. Leonardis, and A. Frisoli, "A new wearable fingertip haptic interface for the rendering of virtual shapes and surface features," in *2016 IEEE Haptics Symposium (HAPTICS)*, 2016, pp. 140–146.

[20] P. Preechayasomboon and E. Rombokas, "Haplets: Finger-worn wireless and low-encumbrance vibrotactile haptic feedback for virtual and augmented reality," *Frontiers in Virtual Reality*, vol. 2, 2021. [Online]. Available: https://www.frontiersin.org/articles/10.3389/frvir.2021.738613

[21] Y. Ujitoko, T. Taniguchi, S. Sakurai, and K. Hirota, "Development of finger-mounted high-density pin-array haptic display," *IEEE Access*, vol. 8, pp. 145 107–145 114, 2020.

[22] V. Shen, T. Rae-Grant, J. Mullenbach, C. Harrison, and C. Shultz, "Fluid reality: High-resolution, untethered haptic gloves using electroosmotic pump arrays," in *Proceedings of the 36th Annual ACM Symposium on User Interface Software and Technology*, 2023, pp. 1–20.

[23] G. Jansson and L. Monaci, "Identification of real objects under conditions similar to those in haptic displays: providing spatially distributed information at the contact areas is more important than increasing the number of areas," *Virtual Reality*, vol. 9, pp. 243–249, 2006.

[24] C. Tzafestas, "Whole-hand kinesthetic feedback and haptic perception in dextrous virtual manipulation," *IEEE Transactions on Systems, Man, and Cybernetics - Part A: Systems and Humans*, vol. 33, no. 1, pp. 100–113, 2003.

[25] A. J. Silva, O. A. D. Ramirez, V. P. Vega, and J. P. O. Oliver, "Phantom omni haptic device: Kinematic and manipulability," in *2009 Electronics, Robotics and Automotive Mechanics Conference (CERMA)*, 2009, pp. 193–198.

[26] N. Technologies, "Novint falcon," 2024, retrieved May 1, 2024 from https://hapticshouse.com/pages/novints-falcon-haptic-device.

[27] F. Dimension, "delta.3," 2024, retrieved May 1, 2024 from https://www.forcedimension.com/products/delta.

[28] H. Culbertson, J. J. L. Delgado, and K. J. Kuchenbecker, "One hundred data-driven haptic texture models and open-source methods for rendering on 3d objects," in *2014 IEEE haptics symposium (HAPTICS)*. IEEE, 2014, pp. 319–325.

[29] S. Yoshida, Y. Sun, and H. Kuzuoka, "Pocopo: Handheld pin-based shape display for haptic rendering in virtual reality," in *Proceedings of the 2020 CHI Conference on Human Factors in Computing Systems*, ser. CHI '20. New York, NY, USA: Association for Computing Machinery, 2020, p. 1–13. [Online]. Available: https://doi.org/10.1145/3313831.3376358

[30] E. Whitmire, H. Benko, C. Holz, E. Ofek, and M. Sinclair, "Haptic revolver: Touch, shear, texture, and shape rendering on a reconfigurable virtual reality controller," in *Proceedings of the 2018 CHI conference on human factors in computing systems*, 2018, pp. 1–12.

[31] I. Choi, H. Culbertson, M. R. Miller, A. Olwal, and S. Follmer, "Grabity: A wearable haptic interface for simulating weight and grasping in virtual reality," in *Proceedings of the 30th Annual ACM Symposium on User Interface Software and Technology*, ser. UIST '17. New York, NY, USA: Association for Computing Machinery, 2017, p. 119–130. [Online]. Available: https://doi.org/10.1145/3126594.3126599

[32] E. J. Gonzalez, E. Ofek, M. Gonzalez-Franco, and M. Sinclair, "X-rings: A hand-mounted 360 shape display for grasping in virtual reality," in *The 34th Annual ACM Symposium on User Interface Software and Technology*, 2021, pp. 732–742.

[33] C. Pacchierotti, S. Sinclair, M. Solazzi, A. Frisoli, V. Hayward, and D. Prattichizzo, "Wearable haptic systems for the fingertip and the hand: taxonomy, review, and perspectives," *IEEE transactions on haptics*, vol. 10, no. 4, pp. 580–600, 2017.

[34] M. Bouzit, G. Burdea, G. Popescu, and R. Boian, "The rutgers master ii-new design force-feedback glove," *IEEE/ASME Transactions on mechatronics*, vol. 7, no. 2, pp. 256–263, 2002.

[35] M. Jo, D. Kwak, and S. H. Yoon, "Wrimoucon: Wrist-mounted haptic controller for rendering physical properties in virtual reality," in *2023 IEEE World Haptics Conference (WHC)*. IEEE, 2023, pp. 34–40.

[36] E. Pezent, A. Israr, M. Samad, S. Robinson, P. Agarwal, H. Benko, and N. Colonnese, "Tasbi: Multisensory squeeze and vibrotactile wrist haptics for augmented and virtual reality," in *2019 IEEE World Haptics Conference (WHC)*. IEEE, 2019, pp. 1–6.

[37] Q. Tong, W. Wei, Y. Zhang, J. Xiao, and D. Wang, "Survey on hand-based haptic interaction for virtual reality," *IEEE Transactions on Haptics*, 2023.

[38] V. Vechev, J. Zarate, D. Lindlbauer, R. Hinchet, H. Shea, and O. Hilliges, "Tactiles: Dual-mode low-power electromagnetic actuators for rendering continuous contact and spatial haptic patterns in vr," in *2019 IEEE Conference on Virtual Reality and 3D User Interfaces (VR)*. IEEE, 2019, pp. 312–320.

[39] L. H. Lee, K. Y. Lam, T. Li, T. Braud, X. Su, and P. Hui, "Quadmetric optimized thumb-to-finger interaction for force assisted one-handed text entry on mobile headsets," *Proceedings of the ACM on Interactive, Mobile, Wearable and Ubiquitous Technologies*, vol. 3, no. 3, pp. 1–27, 2019.

[40] L. Fang, T. Müller, E. Pescara, N. Fischer, Y. Huang, and M. Beigl, "Investigating passive haptic learning of piano songs using three tactile sensations of vibration, stroking and tapping," *Proceedings of the ACM on Interactive, Mobile, Wearable and Ubiquitous Technologies*, vol. 7, no. 3, pp. 1–19, 2023.

[41] D. Wang, M. Song, A. Naqash, Y. Zheng, W. Xu, and Y. Zhang, "Toward whole-hand kinesthetic feedback: A survey of force feedback gloves," *IEEE transactions on haptics*, vol. 12, no. 2, pp. 189–204, 2018.

[42] G. Robles-De-La-Torre and V. Hayward, "Force can overcome object geometry in the perception of shape through active touch," *Nature*, vol. 412, no. 6845, pp. 445–448, 2001.

[43] X. Gu, Y. Zhang, W. Sun, Y. Bian, D. Zhou, and P. O. Kristensson, "Dexmo: An inexpensive and lightweight mechanical exoskeleton for motion capture and force feedback in vr," in *Proceedings of the 2016 CHI Conference on Human Factors in Computing Systems*, ser. CHI '16. New York, NY, USA: Association for Computing Machinery, 2016, p. 1991–1995. [Online]. Available: https://doi.org/10.1145/2858036.2858487

[44] I. Sarakoglou, A. Brygo, D. Mazzanti, N. G. Hernandez, D. G. Caldwell, and N. G. Tsagarakis, "Hexotrac: A highly under-actuated hand exoskeleton for finger tracking and force feedback," in *2016 IEEE/RSJ International Conference on Intelligent Robots and Systems (IROS)*. IEEE, 2016, pp. 1033–1040.

[45] S. Baik, S. Park, and J. Park, "Haptic glove using tendon-driven soft robotic mechanism," *Frontiers in Bioengineering and Biotechnology*, vol. 8, 2020. [Online]. Available: https://www.frontiersin.org/articles/10.3389/fbioe.2020.541105

[46] S. Das, Y. Kishishita, T. Tsuji, C. Lowell, K. Ogawa, and Y. Kurita, "Forcehand glove: A wearable force-feedback glove with pneumatic artificial muscles (pams)," *IEEE Robotics and Automation Letters*, vol. 3, no. 3, pp. 2416–2423, 2018.

[47] M. Hosseini, A. Sengül, Y. Pane, J. De Schutter, and H. Bruyninck, "Exoten-glove: A force-feedback haptic glove based on twisted string actuation system," in *2018 27th IEEE International Symposium on Robot and Human Interactive Communication (RO-MAN)*, 2018, pp. 320–327.

[48] S. H. Winter and M. Bouzit, "Use of magnetorheological fluid in a force feedback glove," *IEEE Transactions on Neural Systems and Rehabilitation Engineering*, vol. 15, no. 1, pp. 2–8, 2007.

[49] J. Blake and H. B. Gurocak, "Haptic glove with mr brakes for virtual reality," *IEEE/ASME Transactions on Mechatronics*, vol. 14, no. 5, pp. 606–615, 2009.

[50] W. Nozaki, K. Koyanagi, T. Oshima, T. Matsuno, and N. Momose, "Development of passive force display glove system and its improved mechanism," in *2007 International Conference on Mechatronics and Automation*. IEEE, 2007, pp. 2645–2650.

[51] HaptX, "Haptx," 2023, retrieved May 1, 2024 from https://haptx.com/.

[52] I. Choi, N. Corson, L. Peiros, E. W. Hawkes, S. Keller, and S. Follmer, "A soft, controllable, high force density linear brake utilizing layer jamming," *IEEE Robotics and Automation Letters*, vol. 3, no. 1, pp. 450–457, 2017.

[53] J. Edwards, B. Jayawant, W. Dawson, and D. Wright, "Permanent-magnet linear eddy-current brake with a non-magnetic reaction plate," *IEE Proceedings-Electric Power Applications*, vol. 146, no. 6, pp. 627–631, 1999.

[54] R. Nith, S.-Y. Teng, P. Li, Y. Tao, and P. Lopes, "Dextrems: Increasing dexterity in electrical muscle stimulation by combining it with brakes," in *The 34th annual ACM symposium on user interface software and technology*, 2021, pp. 414–430.

[55] J. Qi, F. Gao, G. Sun, J. C. Yeo, and C. T. Lim, "Haptglove—untethered pneumatic glove for multimode haptic feedback in reality–virtuality continuum," *Advanced Science*, vol. 10, no. 25, p. 2301044, 2023. [Online]. Available: https://onlinelibrary.wiley.com/doi/abs/10.1002/advs.202301044

[56] R. Hinchet and H. Shea, "High force density textile electrostatic clutch," *Advanced Materials Technologies*, vol. 5, no. 4, 2019.

[57] S. Park, J. Shintake, Y. Piskarev, Y. Wei, I. Joshipura, E. Frey, T. Neumann, D. Floreano, and M. D. Dickey, "Stretchable and soft electroadhesion using liquid-metal subsurface microelectrodes," *Advanced Materials Technologies*, vol. 6, no. 9, p. 2100263, 2021.

[58] V. Ramachandran, J. Shintake, and D. Floreano, "All-fabric wearable electroadhesive clutch," *Advanced Materials Technologies*, vol. 4, no. 2, p. 1800313, 2019.

[59] A. Mishra, P. Kumar, J. Shukla, and A. Parnami, "Haptidrag: A device with the ability to generate varying levels of drag (friction) effects on real surfaces," *Proceedings of the ACM on Interactive, Mobile, Wearable and Ubiquitous Technologies*, vol. 6, no. 3, pp. 1–26, 2022.

[60] K. Amano and A. Yamamoto, "An interaction on a flat panel display using a planar 1-dof electrostatic actuator," in *Proceedings of the ACM International Conference on Interactive Tabletops and Surfaces*, 2011, pp. 258–259.

[61] H. Prahlad, R. Pelrine, S. Stanford, J. Marlow, and R. Kornbluh, "Electroadhesive robots—wall climbing robots enabled by a novel, robust, and electrically controllable adhesion technology," in *2008 IEEE international conference on robotics and automation*. IEEE, 2008, pp. 3028–3033.

[62] M. Kono, T. Takahashi, H. Nakamura, T. Miyaki, and J. Rekimoto, "Design guideline for developing safe systems that apply electricity to the human body," *ACM Trans. Comput.-Hum. Interact.*, vol. 25, no. 3, jun 2018. [Online]. Available: https://doi.org/10.1145/3184743

[63] J. P. Reilly, *Applied bioelectricity: from electrical stimulation to electropathology.* Springer Science & Business Media, 2012.

[64] B. Son and J. Park, "Haptic feedback to the palm and fingers for improved tactile perception of large objects," in *Proceedings of the 31st Annual ACM Symposium on User Interface Software and Technology*, 2018, pp. 757–763.

[65] P. P. pico Voltron., "Shvps single channel high voltage power supply," retrieved May 1, 2024 from https://petapicovoltron.com/single-channel-high-voltage-power-supply.

[66] R. Johansson and A. Vallbo, "Detection of tactile stimuli. thresholds of afferent units related to psychophysical thresholds in the human hand." *The Journal of physiology*, vol. 297, no. 1, pp. 405–422, 1979.

[67] E. L. Secco and A. M. Tadesse, "A wearable exoskeleton for hand kinesthetic feedback in virtual reality," in *Wireless Mobile Communication and Healthcare*, G. M. O'Hare, M. J. O'Grady, J. O'Donoghue, and P. Henn, Eds. Cham: Springer International Publishing, 2020, pp. 186–200.

[68] S. Sathiyamurthy, M. Lui, E. Kim, and O. Schneider, "Measuring haptic experience: Elaborating the hx model with scale development," in *2021 IEEE World Haptics Conference (WHC)*. IEEE, 2021, pp. 979–984.

[69] P. Boonmee, B. Jantarakongkul, and P. Jitngernmadan, "Vr training environment for electrical vehicle assembly training in eec," in *2020 - 5th International Conference on Information Technology (InCIT)*, 2020, pp. 238–242.

[70] E. Gallegos-Nieto, H. I. Medellín-Castillo, G. González-Badillo, T. Lim, and J. Ritchie, "The analysis and evaluation of the influence of haptic-enabled virtual assembly training on real assembly performance," *The International Journal of Advanced Manufacturing Technology*, vol. 89, no. 1, pp. 581–598, 2017. [Online]. Available: https://doi.org/10.1007/s00170-016-9120-4

[71] C. G. Cao, M. Zhou, D. B. Jones, and S. D. Schwaitzberg, "Can surgeons think and operate with haptics at the same time?" *Journal of Gastrointestinal Surgery*, vol. 11, no. 11, pp. 1564–1569, 2007. [Online]. Available: https://www.sciencedirect.com/science/article/pii/S1091255X23049041

[72] M. Hoppe, B. Rossmy, D. P. Neumann, S. Streuber, A. Schmidt, and T.-K. Machulla, "A human touch: Social touch increases the perceived human-likeness of agents in virtual reality," in *Proceedings of the 2020 CHI conference on human factors in computing systems*, 2020, pp. 1–11.